ICHEP94 Ref. GLS0381
Submitted to PA 16,2 Pl 9,19

CLEO CONF 94-18

Measurement of the ratios $\mathcal{B}(D_s^+ \to \eta\ell^+\nu)/\mathcal{B}(D_s^+ \to \phi\ell^+\nu)$ and $\mathcal{B}(D_s^+ \to \eta'\ell^+\nu)/\mathcal{B}(D_s^+ \to \phi\ell^+\nu)$.

M. Battle,[1] J. Ernst,[1] L. Gibbons,[1] Y. Kwon,[1] S. Roberts,[1] E.H. Thorndike,[1] C.H. Wang,[1] J. Dominick,[2] M. Lambrecht,[2] S. Sanghera,[2] V. Shelkov,[2] T. Skwarnicki,[2] R. Stroynowski,[2] I. Volobouev,[2] G. Wei,[2] P. Zadorozhny,[2] M. Artuso,[3] M. Gao,[3] M. Goldberg,[3] D. He,[3] N. Horwitz,[3] G.C. Moneti,[3] R. Mountain,[3] F. Muheim,[3] Y. Mukhin,[3] S. Playfer,[3] Y. Rozen,[3] S. Stone,[3] X. Xing,[3] G. Zhu,[3] J. Bartelt,[4] S.E. Csorna,[4] Z. Egyed,[4] V. Jain,[4] D. Gibaut,[5] K. Kinoshita,[5] P. Pomianowski,[5] B. Barish,[6] M. Chadha,[6] S. Chan,[6] D.F. Cowen,[6] G. Eigen,[6] J.S. Miller,[6] C. O'Grady,[6] J. Urheim,[6] A.J. Weinstein,[6] M. Athanas,[7] W. Brower,[7] G. Masek,[7] H.P. Paar,[7] J. Gronberg,[8] R. Kutschke,[8] S. Menary,[8] R.J. Morrison,[8] S. Nakanishi,[8] H.N. Nelson,[8] T.K. Nelson,[8] C. Qiao,[8] J.D. Richman,[8] A. Ryd,[8] H. Tajima,[8] D. Sperka,[8] M.S. Witherell,[8] R. Balest,[9] K. Cho,[9] W.T. Ford,[9] D.R. Johnson,[9] K. Lingel,[9] M. Lohner,[9] P. Rankin,[9] J.G. Smith,[9] J.P. Alexander,[10] C. Bebek,[10] K. Berkelman,[10] K. Bloom,[10] T.E. Browder,[10*] D.G. Cassel,[10] H.A. Cho,[10] D.M. Coffman,[10] D.S. Crowcroft,[10] P.S. Drell,[10] D. Dumas,[10] R. Ehrlich,[10] P. Gaidarev,[10] M. Garcia-Sciveres,[10] B. Geiser,[10] B. Gittelman,[10] S.W. Gray,[10] D.L. Hartill,[10] B.K. Heltsley,[10] S. Henderson,[10] C.D. Jones,[10] S.L. Jones,[10] J. Kandaswamy,[10] N. Katayama,[10] P.C. Kim,[10] D.L. Kreinick,[10] G.S. Ludwig,[10] J. Masui,[10] J. Mevissen,[10] N.B. Mistry,[10] C.R. Ng,[10] E. Nordberg,[10] J.R. Patterson,[10] D. Peterson,[10] D. Riley,[10] S. Salman,[10] M. Sapper,[10] F. Würthwein,[10] P. Avery,[11] A. Freyberger,[11] J. Rodriguez,[11] S. Yang,[11] J. Yelton,[11] D. Cinabro,[12] T. Liu,[12] M. Saulnier,[12] R. Wilson,[12] H. Yamamoto,[12] T. Bergfeld,[13] B.I. Eisenstein,[13] G. Gollin,[13] B. Ong,[13] M. Palmer,[13] M. Selen,[13] J. J. Thaler,[13] K.W. Edwards,[14] M. Ogg,[14] A. Bellerive,[15] D.I. Britton,[15] E.R.F. Hyatt,[15] D.B. MacFarlane,[15] P.M. Patel,[15] B. Spaan,[15] A.J. Sadoff,[16] R. Ammar,[17] P. Baringer,[17] A. Bean,[17] D. Besson,[17] D. Coppage,[17] N. Copty,[17] R. Davis,[17] N. Hancock,[17] M. Kelly,[17] S. Kotov,[17] I. Kravchenko,[17] N. Kwak,[17] H. Lam,[17] Y. Kubota,[18] M. Lattery,[18] M. Momayezi,[18] J.K. Nelson,[18] S. Patton,[18] R. Poling,[18] V. Savinov,[18] S. Schrenk,[18] R. Wang,[18] M.S. Alam,[19] I.J. Kim,[19] Z. Ling,[19] A.H. Mahmood,[19] J.J. O'Neill,[19] H. Severini,[19] C.R. Sun,[19] F. Wappler,[19] G. Crawford,[20] C. M. Daubenmier,[20] R. Fulton,[20] D. Fujino,[20] K.K. Gan,[20] K. Honscheid,[20] H. Kagan,[20] R. Kass,[20] J. Lee,[20] R. Malchow,[20] Y. Skovpen,[20†] M. Sung,[20] C. White,[20] M.M. Zoeller,[20] F. Butler,[21] X. Fu,[21] B. Nemati,[21] W.R. Ross,[21] P. Skubic,[21] M. Wood,[21] M. Bishai,[22] J. Fast,[22] E. Gerndt,[22] R.L. McIlwain,[22] T. Miao,[22] D.H. Miller,[22] M. Modesitt,[22] D. Payne,[22] E.I. Shibata,[22] I.P.J. Shipsey,[22] and P.N. Wang[22]

(CLEO Collaboration)

[1] *University of Rochester, Rochester, New York 14627*
[2] *Southern Methodist University, Dallas, Texas 75275*
[3] *Syracuse University, Syracuse, New York 13244*
[4] *Vanderbilt University, Nashville, Tennessee 37235*
[5] *Virginia Polytechnic Institute and State University, Blacksburg, Virginia, 24061*
[6] *California Institute of Technology, Pasadena, California 91125*
[7] *University of California, San Diego, La Jolla, California 92093*
[8] *University of California, Santa Barbara, California 93106*
[9] *University of Colorado, Boulder, Colorado 80309-0390*
[10] *Cornell University, Ithaca, New York 14853*
[11] *University of Florida, Gainesville, Florida 32611*
[12] *Harvard University, Cambridge, Massachusetts 02138*
[13] *University of Illinois, Champaign-Urbana, Illinois, 61801*
[14] *Carleton University, Ottawa, Ontario K1S 5B6 and the Institute of Particle Physics, Canada*
[15] *McGill University, Montréal, Québec H3A 2T8 and the Institute of Particle Physics, Canada*
[16] *Ithaca College, Ithaca, New York 14850*
[17] *University of Kansas, Lawrence, Kansas 66045*
[18] *University of Minnesota, Minneapolis, Minnesota 55455*
[19] *State University of New York at Albany, Albany, New York 12222*
[20] *Ohio State University, Columbus, Ohio, 43210*
[21] *University of Oklahoma, Norman, Oklahoma 73019*
[22] *Purdue University, West Lafayette, Indiana 47907*

Abstract

Using the CLEO II detector at the Cornell Electron Storage Ring (CESR), we have investigated the decays, $D_s^+ \to \eta\ell^+\nu$ and $D_s^+ \to \eta'\ell^+\nu$. We observe clean signatures in $\eta \to \gamma\gamma$ and $\eta' \to \eta\pi^+\pi^-$ and normalize these yields to the yield in the vector channel $D_s^+ \to \phi\ell^+\nu$. We have measured $\mathcal{B}(D_s^+ \to \eta e^+\nu)/\mathcal{B}(D_s^+ \to \phi e^+\nu) = 1.74 \pm 0.34 \pm 0.24$, $\mathcal{B}(D_s^+ \to \eta' e^+\nu)/\mathcal{B}(D_s^+ \to \phi e^+\nu) = 0.71^{+0.19+0.08}_{-0.18-0.10}$.

---

*Permanent address: University of Hawaii at Manoa

†Permanent address: INP, Novosibirsk, Russia

Heavy quark semileptonic decays are theoretically straightforward to interpret since the amplitude for such decays can be factorized into a product of leptonic and hadronic currents. Measurements of the ratio of pseudoscalar to vector rates for D mesons disagree with theoretical expectations. For example, the experimental world average for $\mathcal{B}(D \to K\ell^+\nu)/\mathcal{B}(D \to \overline{K^*}\ell^+\nu)$ is 1.75±0.15 [1–3] whereas theoretical predictions range from 0.8 to 1.4 [4–8]. It is of interest to repeat these types of measurements using D_s mesons. In this paper we report the first measurements of $\mathcal{B}(D_s^+ \to \eta\ell^+\nu)$ and $\mathcal{B}(D_s^+ \to \eta'\ell^+\nu)$. We compare these measurements with $\mathcal{B}(D_s^+ \to \phi\ell^+\nu)$ and determine the pseudoscalar to vector ratio for D_s^+ semileptonic decays.

Due to the undetected neutrino, we cannot fully reconstruct $D_s^+ \to X\ell^+\nu$ ($X = \phi, \eta, \eta'$) decays. However, there are few processes which produce both a ϕ, η or η' meson and a lepton contained in the same jet. Consequently, this correlation can be used to extract a clean $D_s^+ \to X\ell^+\nu$ signal. The backgrounds due to misidentified leptons and from random X–lepton combinations can be reliably estimated, and the possible contamination from other decay modes can be shown to be small.

We extract the yields of $D_s^+ \to \eta\ell^+\nu$ and $D_s^+ \to \phi\ell^+\nu$ events using a D_s^{*+} tag and measure $\mathcal{B}(D_s^+ \to \eta\ell^+\nu)/\mathcal{B}(D_s^+ \to \phi\ell^+\nu)$. We use the D_s^{*+} tag to reduce the random η-lepton background. In a separate analysis, we extract the yields of $D_s^+ \to \eta'\ell^+\nu$ and $D_s^+ \to \phi\ell^+\nu$ events without the D_s^{*+} tag and measure $\mathcal{B}(D_s^+ \to \eta'\ell^+\nu)/\mathcal{B}(D_s^+ \to \phi\ell^+\nu)$.

The data consists of an integrated luminosity of 2.35 fb^{-1} of e^+e^- collisions recorded with the CLEO II detector at the Cornell Electron Storage Ring (CESR). A detailed description of the CLEO II detector can be found in reference [10]. The data sample contains about three million $e^+e^- \to c\bar{c}$ events taken at center-of-mass energies on the $\Upsilon(4S)$ resonance and in the nearby continuum ($\sqrt{s} \sim 10.6$ GeV). The CLEO II detector is ideally suited to detect the decay chain $D_s^{*+} \to D_s^+\gamma$, $D_s^+ \to \eta\ell^+\nu$ or $D_s^+ \to \eta'\ell^+\nu$ due to the excellent CsI crystal calorimeter.

We identify ϕ candidates by using the decay mode $\phi \to K^+K^-$. The charged kaon candidates must have the ionization energy loss and time-of-flight consistent with what we expect for true kaons.

We use the decay mode $\eta \to \gamma\gamma$ to select η candidates. The photon candidates are restricted to lie in the fiducial region, $|\cos\theta| < 0.81$, where θ is the polar angle of the track with respect to the beam axis. We require that $|\cos\theta_{decay}| < 0.9$, where θ_{decay} is the photon decay angle in the η rest frame with respect to the η direction in the laboratory. Backgrounds due to low momentum photons tend to peak at $|\cos\theta_{decay}| = 1$. Since most photons are daughters of π^0 decays, we eliminate any photon which, combined with another photon, makes a mass combination consistent with π^0 mass ($\pm 2.5\sigma$) and has a π^0 momentum greater than 0.8 GeV/c.

We identify η' candidates via the decay chain $\eta' \to \eta\pi^+\pi^-$, $\eta \to \gamma\gamma$ with the selection of η candidates as explained above. The charged pion candidates must have the ionization energy loss and time-of-flight consistent with what we expect for true pions.

Lepton candidates are restricted to the kinematic regions in which the lepton identification efficiencies and hadron misidentification rates are well understood. Hence, electron and muon candidates are restricted to lie in the fiducial regions $|\cos\theta| < 0.91$ and $|\cos\theta| < 0.81$, respectively. In addition, electron candidates must have momenta above 0.7 GeV/c and muon candidates above 1.5 GeV/c. The only exception is for muons in the

region $|\cos\theta| > 0.61$ which are required to have momenta above 1.9 GeV/c. Electrons are identified by comparing their ionization energy loss, time-of-flight, and energy deposited in the electromagnetic calorimeter with what we expect for true electrons. Electrons from photon conversions and Dalitz decays of π^0's are rejected by pairing electron candidates with all other oppositely charged tracks in the event and rejecting those which have both small separation and parallel trajectories at their point of closest approach. Muons are identified by matching charged tracks to hits in the muon detectors. In order to be identified as a muon, a track must penetrate at least 5 interaction lengths of iron.

We require that the momentum of η candidates be greater than 1.0 GeV/c to suppress the combinatoric background. In order to be consistent with having originated from a D_s^+ decay, the $\eta\ell^+$ candidates must have an invariant mass less than 1.9 GeV/c^2 and greater than 1.2 GeV/c^2. In addition, we require that the $\eta\ell^+$ momentum be greater than 2.0 GeV/c to reduce random $\eta\ell^+$ combinations. In order to suppress the combinatoric background from $\Upsilon(4S)$ events, which tend to be more spherical, we require the ratio of Fox-Wolfram moments [12], $R_2 = H_2/H_0$, to be greater than 0.30.

After selecting $\eta\ell^+$ candidates which pass the above criteria, we then combine them with a photon which lies in the same hemisphere. The photon must lie in the fiducial region, $|\cos\theta| < 0.71$, and have the energy greater than 0.12 GeV. To further suppress background photons from π^0 decays, we veto all $\gamma\gamma$ combinations that fall within 2.5σ of the π^0 mass.

Assuming the D_s^{*+} direction is along the thrust axis, the momentum of the D_s^{*+} can be estimated from the photon momentum and the thrust axis direction. We require that the β of D_s^{*+} be between 0.58 and 0.97, which optimizes the signal-to-background ratio.

To select $\eta\ell^+\gamma$ candidates which come from the $D_s^{*+} \to D_s^+\gamma$, $D_s^+ \to \eta\ell^+\nu$ decay chain, we require that $\Delta M \equiv M_{\eta\ell\gamma} - M_{\eta\ell}$ be between 0.1 and 0.2 GeV/c^2 where $M_{\eta\ell}$ and $M_{\eta\ell\gamma}$ are the invariant masses of $\eta\ell^+$ and $\eta\ell^+\gamma$ systems, respectively.

The efficiency for reconstructing $D_s^+ \to \eta\ell^+\nu$ decay is obtained from a Monte Carlo simulation which uses the predictions of the ISGW model [4] as input. These events are then passed through a full simulation of the CLEO II detector and the same event reconstruction and analysis chain as the data. Following the above selection criteria, and after correcting for the effects of final-state radiation from the leptons [13], the efficiency to identify the $D_s^+ \to \eta\ell^+\nu$ decay is 0.94%.

Figure 1 shows the $\gamma\gamma$ invariant mass distribution for all $\eta\ell^+\gamma$ combinations which pass the above selection criteria. We fit these distributions with a signal and background function. The signal function is a asymmetric Gaussian function. The background function is a second order Chebyshev polynomial function which accounts for random $\gamma\gamma$ combinations. The mean and sigmas of the Gaussian function are fixed to the values extracted from a fit to all η candidates with momenta above 1.0 GeV/c. The fit yields 103.0 ± 11.9 $D_s^+ \to \eta\ell^+\nu$ candidates.

There are three main sources of background in the sample: η's accompanied by fake leptons [14], random $\eta\ell^+$ combinations, and random photon combinations. The background due to fake leptons is estimated by first using the real data to measure the momentum dependent probabilities that a hadron will be misidentified as a lepton. These probabilities are typically 0.3% for electrons and 1.2% for muons. We use all charged tracks in the event which do not pass the lepton identification criteria described above and treat them as leptons. The number of the events which pass our cuts are multiplied by the fake probability

to find total number of fake lepton events. With this procedure, we estimate the number of $\eta\ell^+$ combinations due to misidentified hadrons to be 13.7 ± 4.1 events. The quoted error includes the contributions from the uncertainties in the misidentification probabilities.

For the range of lepton momenta considered, random $\eta\ell^+$ combinations come from two sources: from $e^+e^- \to c\bar{c}$ events in which an η produced in the fragmentation process is combined with a lepton from a semileptonic decay of the charmed hadron in the same jet, and from $\Upsilon(4S) \to B\bar{B}$ events in which an η is produced in the decay chain of one of the B mesons is combined with a lepton from the semileptonic decay of the other B meson. The background from random $\eta\ell^+$ combinations is estimated using the Monte Carlo simulation. However, the η production rate from both fragmentation and B meson decays is not well known. For this reason, an attempt is made to scale the Monte Carlo prediction to account for the η production rate observed in the data.

In the charm continuum events, leptons come primarily from the charm semileptonic decays. Therefore the direction of a charmed hadron is close to that of the high momentum lepton. In the charm continuum events, not only the rate of η production, but also the correlation between the η and the charmed hadron direction is important. The agreement between the data and the Monte Carlo simulation is investigated by considering how often an η is produced in the same hemisphere as a fully reconstructed D meson. Both D^0 and D^{*+} mesons are considered, and are reconstructed using the following decay chains: $D^0 \to K^-\pi^+$ and $D^{*+} \to D^0\pi^+$, $D^0 \to K^-\pi^+$. The reconstructed D mesons are required to have momenta above 2.5 GeV/c in order to account for the range of D momenta which are expected to contribute leptons in the momentum range of interest. For this particular study, the η momentum criterion is relaxed to 0.8 GeV/c in order to provide sufficient statistics. In doing this we have assumed that the η momentum distribution is well reproduced by the Monte Carlo simulation, and that it is the rate of η production in the fragmentation process which contributes the greatest uncertainty. The yields of D mesons and η mesons are obtained by fitting their invariant mass distributions. D meson combinatoric backgrounds are accounted for by subtracting the number of η's found when using the D meson invariant mass sidebands. In data 1.2 ± 0.5 η mesons are found for every 1000 reconstructed D mesons. This is to be compared with 1.7 ± 0.1 in the $e^+e^- \to c\bar{c}$ Monte Carlo sample. The ratio of these two numbers is 0.7 ± 0.3. With this scaling factor, the simulation predicts a charm continuum background of 12 ± 5 events, where the error includes the uncertainty in the above ratio.

The background from random $\eta\ell^+$ combinations from $B\bar{B}$ events is estimated in a similar manner. In this case the directions of the η and lepton are uncorrelated. For this reason it is sufficient to compare the number of η's with momentum above 1.0 GeV/c in the continuum subtracted $\Upsilon(4S)$ data with what we observe in the $\Upsilon(4S)$ $B\bar{B}$ Monte Carlo sample. In data 7.4 ± 0.8 η's are found for every 1000 $B\bar{B}$ events, which is to be compared with 6.4 ± 0.1 in the $B\bar{B}$ Monte Carlo sample. This gives a scaling factor of 1.1 ± 0.1. After applying this correction, the predicted background from $B\bar{B}$ events is 1.7 ± 0.2 events.

We have also estimated the possible contamination from the decays $D_s^+ \to \eta'\ell^+\nu$, $D^+ \to \eta\ell^+\nu$ and $D^+ \to \eta'\ell^+\nu$. For $D_s^+ \to \eta'\ell^+\nu$ decay, we estimate the efficiency using the Monte Carlo simulation. Due to the hard momentum cut for η and the $M_{\eta\ell^+} > 1.2$ GeV/c^2 cut, the efficiency is found to be very small, 0.11%, which is 1/9 of that for $D_s^+ \to \eta\ell^+\nu$ decay. We have 6100^{+1600}_{-1500} $D_s^+ \to \eta'\ell^+\nu$ events in our data sample as discussed below. Considering

the branching fractions for $\eta' \to \eta X$ and $\eta \to \gamma\gamma$ and the fact that a half of D_s yields comes from D_s^*, we estimate 1.2 ± 0.4 events from the $D_s^+ \to \eta'\ell^+\nu$ feed down. The contamination from the decays $D^+ \to \eta\ell^+\nu$ and $D^+ \to \eta'\ell^+\nu$ are negligible since the decay modes are Cabibbo suppressed modes and $\mathcal{B}(D^{*+} \to D^+\gamma)$ is small.

The background from the combinations of true $\eta\ell^+$'s and random photons is estimated using a Monte Carlo simulation. To scale the Monte Carlo estimate for the random photon background to data, we investigate how often a K^-e^+ combination from the decay chain, $D^{*+} \to D^0\pi^+$ and $D^0 \to K^-e^+\nu$, combines with random photons and passes the cuts we impose. For this investigation, we first reconstruct the decay chain, $D^{*+} \to D^0\pi^+$ and $D^0 \to K^-e^+\nu$ by applying the same cuts for selecting K^-e^+ combinations as for $D_s^+ \to \eta\ell^+\nu$ candidates and fitting the pseudo mass difference $M_{K^-e^+\pi^+} - M_{K^-e^+}$ distribution. We find 5000 ± 72 K^-e^+ combinations in the Monte Carlo sample and 1677 ± 44 in the data sample. Then we add random photons to the K^-e^+ combinations and calculate $\beta_{D_s^{*+}}$ and ΔM as described for the $D_s^+ \to \eta\ell^+\nu$ analysis. Finally we refit the pseudo mass difference $M_{K^-e^+\pi^+} - M_{K^-e^+}$ distribution in the signal region and the grand sideband, where the signal region satisfies both $0.1 < \Delta M < 0.2$ and $0.58 < \beta_{D_s^{*+}} < 0.97$ while the grand sideband is outside the signal region. In the signal region the refit gives 242.1 ± 15.6 K^-e^+ combinations for the Monte Carlo sample and 82.8 ± 10.3 for the data sample. Therefore, the probability to have random photon background in the signal region is $4.8 \pm 0.3\%$ for the Monte Carlo and $4.9 \pm 0.6\%$ for the data. The scaling factor for the signal region is 1.02 ± 0.15. In the same manner we find the scaling factor for the grand sideband to be 1.15 ± 0.09. Since two scaling factors are consistent, we combine these scaling factors to find the overall scaling factor for the random photon background and obtain 1.11 ± 0.08. With this scaling factor, the Monte Carlo simulation predicts the ratio of the random photon background to the sum of the signal and the random photon background, f_{RD}, to be 0.188 ± 0.066 in our data sample after fake lepton, $B\bar{B}$, $c\bar{c}$ and $D_s^+ \to \eta'\ell^+\nu$ feed down backgrounds are subtracted.

Fig 2 shows the number of η's which fall in each ΔM bin. The combined background estimate is also shown, as well as the simulated prediction for the signal shape which has been normalized to the number of candidates extracted from the fit to the $\gamma\gamma$ invariant mass spectrum. The predicted signal shape is in good agreement with the data. The background estimate can be checked by comparing the predicted number of candidates with the observed number in the grand sideband. We predict 109.9 ± 14.6 events and observe 100.3 ± 13.1 in the grand sideband. The prediction is in good agreement with the observation.

We calculate a final signal yield as $N_{signal} = (N_{observed} - N_{fake\ lepton} - N_{c\bar{c}} - N_{B\bar{B}} - N_{feed\ down}) \times (1 - f_{RD})$. After subtracting all backgrounds, we find 60.9 ± 9.7 $D_s^+ \to \eta\ell^+\nu$ events. After correcting for the detection efficiency and for the $\eta \to \gamma\gamma$ branching fraction [3], the efficiency corrected yield for $D_s^+ \to \eta\ell^+\nu$ is 8320 ± 1320 events. We have taken into account the 3% reduction of the muon rate relative to the electron rate due to phase-space [15]. Therefore, our result is given in terms of the effective yield in the electron channel.

In order to minimize the systematic error from the selection criteria, the number of $D_s^+ \to \phi\ell^+\nu$ decays is measured in a similar manner. The ϕ candidates are required to have momenta above 1.0 GeV/c . Because of the small q^2 value associated with the decay $\phi \to K^+K^-$, the kaons tend to overlap in the drift-chamber. This makes it difficult to simulate accurately the ionization energy loss measurement. In order to avoid this problem,

TABLE I. Summary of $D_s^+ \to \eta\ell^+\nu$ and $D_s^+ \to \phi\ell^+\nu$ yields. The errors quoted in this table are statistical only.

Decay mode	$D_s^+ \to \eta\ell^+\nu$	$D_s^+ \to \phi\ell^+\nu$
Total candidates	103.0 ± 11.9	167.9 ± 15.8
Fake lepton background	13.7 ± 0.6	14.5 ± 0.7
Continuum $c\bar{c}$ background	11.5 ± 1.1	8.8 ± 0.4
$B\bar{B}$ background	1.7 ± 0.4	3.4 ± 0.4
Feed down from $D_s^+ \to \eta'\ell^+\nu$	1.2 ± 0.4	0.0
f_{RD}	0.188	0.255
Signal yield	60.9 ± 9.7	105.3 ± 11.8
Efficiency, $\epsilon \cdot \mathcal{B}$ (%)	0.366	1.104
Efficiency corrected yield	8320 ± 1320	4770 ± 530

the momentum dependent efficiencies for identifying ϕ mesons are obtained from the data by comparing the inclusive yield of all ϕ's before and after particle identification. These efficiencies are then combined with the predicted ϕ momentum spectrum from $D_s^+ \to \phi\ell^+\nu$ decays to give the total ϕ identification efficiency. The efficiency for detecting $D_s^+ \to \phi\ell^+\nu$ decays following these selection criteria is 2.25%.

Fig 3 shows the K^+K^- invariant mass distribution for all $\phi\ell^+\gamma$ combinations which pass the above selection criteria. We fit these distributions with a signal and background function. The signal function is a Gaussian function convoluted with a Breit-Wigner function. The background function is a phase-space background function [16] which accounts for random K^+K^- combinations. The width of the Breit-Wigner function is fixed to the natural width of the ϕ state [3], and the mean and sigma of the Gaussian function are fixed to the values extracted from a fit to all ϕ candidates with momenta above 1.0 GeV/c. Only the overall normalization of the signal function is allowed to vary in the fits. We find 167.9 ± 15.8 $D_s^+ \to \phi\ell^+\nu$ candidates. After subtracting all backgrounds in same manner as $D_s^+ \to \eta\ell^+\nu$ analysis, the efficiency corrected yield is 4770 ± 530 events.

Fig 4 shows the number of ϕ's which fall in each ΔM bin. The combined background estimate is also shown, as well as the simulated prediction for the signal shape which has been normalized to the number of candidates extracted from the fit to the K^+K^- invariant mass spectrum. The background estimate can be checked by comparing the predicted number of candidates with the observed number in the grand sideband. We predict 197 ± 19 events and observe 195 ± 20 in the grand sideband. The prediction is in good agreement with the observation.

Table I summarizes the results for both $D_s^+ \to \eta\ell^+\nu$ and $D_s^+ \to \phi\ell^+\nu$ decays. Since we have already corrected for efficiencies, the ratio of branching fractions is,

$$R_\eta = \frac{\mathcal{B}(D_s^+ \to \eta e^+\nu)}{\mathcal{B}(D_s^+ \to \phi e^+\nu)} = \frac{8320 \pm 1320}{4770 \pm 530} = 1.74 \pm 0.34 \pm 0.24, \qquad (1)$$

where the first error is statistical, and the second is an estimate of systematic effects. This systematic error includes: the uncertainty in the number of fake leptons (2.4%), the uncertainty in the level of continuum charm background (8.2%), the uncertainty in the level of $B\bar{B}$ background (0.3%), the uncertainty in the tracking efficiency (4.0%), the uncertainty in the ϕ identification efficiency (3.0%), the uncertainty in the η reconstruction efficiency (5.0%), the uncertainty in the estimate of random photon background (2.4%), the uncertainty in the estimate of $D_s^+ \to \eta'\ell^+\nu$ feed down (0.5%) and that due to the limited number of Monte Carlo events which were used for the efficiency estimates (6.7%). Various background shapes have also been used to extract the number of η and ϕ mesons. In all cases the results changes by less than 5.8%, which is taken to be the systematic error. Note that systemtics associated with the rate of fake leptons and the scaling of the random photo background mostly cancel since they are correlated in both analyses. After adding these estimates in quadrature, the total systematic error is 14%.

Having measured the ratio $\mathcal{B}(D_s^+ \to \eta e^+\nu)/\mathcal{B}(D_s^+ \to \phi e^+\nu)$, we now turn to the ratio $\mathcal{B}(D_s^+ \to \eta' e^+\nu)/\mathcal{B}(D_s^+ \to \phi e^+\nu)$. We reconstruct η' with the decay chain $\eta' \to \eta\pi^+\pi^-$, $\eta \to \gamma\gamma$. The momenta of η and η' candidates are required to be greater than 0.6 and 1.0 GeV/c, respectively in order to reduce combinatoric background. We do not use the D_s^{*+} tag for the $D_s^+ \to \eta'\ell^+\nu$ analysis since the sensitivity for the η' decay chain is 1/5 of that for the $\eta \to \gamma\gamma$ decay. To compensate for the absence of the D_s^{*+} constraint, we apply tighter cuts than those used for $D_s^+ \to \eta\ell^+\nu$ analysis.

To reduce the random $\eta'\ell^+$ combinations, we require that $P_{\eta'\ell^+}$ be greater than 3.0 GeV/c. To reduce the fake lepton background as well as random $\eta'\ell^+$ combinations, we require that electron momentum be greater than 1.0 GeV/c. Other cuts are same as $D_s^+ \to \eta\ell^+\nu$ analysis. The efficiencies for reconstructing $D_s^+ \to \eta'\ell^+\nu$ decay is 1.11%. The pion identification efficiency is obtained from data in the same manner as the kaon identification efficiency for ϕ reconstruction.

Fig 5 shows the invariant mass distribution of all $\eta\pi^+\pi^-$ combinations which pass the above selection criteria. We fit these distributions with a signal and background function. The signal function is a Gaussian function. The background function is a first order polynomial function which accounts for random $\eta\pi^+\pi^-$ combinations. The mean and sigma of the Gaussian function are fixed to the values extracted from a fit to all η' candidates with momenta above 1.0 GeV/c. The fits yield $29.1^{+6.2}_{-5.6}$ $D_s^+ \to \eta'\ell^+\nu$ candidates. There are two main sources of background: η''s accompanied by fake leptons and random $\eta'\ell^+$ combinations.

The backgrounds are estimated in the same manner as the $D_s^+ \to \eta\ell^+\nu$ analysis. We estimate the background due to fake leptons to be 5.2 ± 1.5. We estimate the random $\eta'\ell^+$ combination background using the Monte Carlo simulation. The scaling factor is measured to be $0.0^{+0.4}_{-0.0}$ for $c\bar{c}$ background and 0.3 ± 0.2 for $B\bar{B}$ background. The resulting estimates for $c\bar{c}$ and $B\bar{B}$ backgrounds are $0.0^{+0.2}_{-0.0}$ events and 0.7 ± 0.6 events, respectively.

We estimate possible feed down from $D^+ \to \eta'\ell^+\nu$, which is relatively large since we do not distinguish D_s^+ from D^+ unlike the $D_s^+ \to \eta\ell^+\nu$ analysis which uses the D_s^{*+} tag. We estimate the ratio of the number of $D^+ \to \eta'\ell^+\nu$ events to the number of $D_s^+ \to \eta'\ell^+\nu$ events, $N(D^+ \to \eta'\ell^+\nu)/N(D_s^+ \to \eta'\ell^+\nu) = 0.06 \pm 0.04$ [17]. We calculate the final signal yield for $D_s^+ \to \eta'\ell^+\nu$ decay as $N_{final} = (N_{observed} - N_{fake\ lepton} - N_{c\bar{c}} - N_{B\bar{B}}) \times 1/(1+f_{FD})$ and obtain $21.9^{+5.8}_{-5.3}$ events. After correcting for the detection efficiencies and for the $\eta' \to \eta\pi^+\pi^-$, $\eta \to \gamma\gamma$ branching fractions [3], the efficiency corrected yield for $D_s^+ \to \eta'\ell^+\nu$ is 6100^{+1600}_{-1500}.

For the $D_s^+ \to \phi\ell^+\nu$ analysis, we apply the same cuts as in the $D_s^+ \to \eta'\ell^+\nu$ analysis to minimize the systematic effects. The result of the fit to the K^+K^- invariant mass distribu-

tion is shown in Fig. 6. We find 419 ± 24 candidates. After subtracting all backgrounds, the efficiency corrected yield for $D_s^+ \to \phi\ell^+\nu$ decay is 8580 ± 600 events. Table II summarize

TABLE II. Summary of $D_s^+ \to \eta'\ell^+\nu$ and $D_s^+ \to \phi\ell^+\nu$ yields. The errors quoted in this table are statistical only.

Decay mode	$D_s^+ \to \eta'\ell^+\nu$	$D_s^+ \to \phi\ell^+\nu$
Total candidates	$29.1^{+6.2}_{-5.6}$	419 ± 24
Fake lepton background	5.2 ± 0.3	50 ± 1.0
Continuum $c\bar{c}$ background	0.0 ± 0.2	6.6 ± 0.3
$B\bar{B}$ background	0.7 ± 0.1	1.7 ± 0.8
f_{FD}	0.06	0.0
Signal yield	$21.9^{+5.8}_{-5.3}$	345 ± 24
Efficiency, $\epsilon \cdot \mathcal{B}$ (%)	0.18	2.01
Efficiency corrected yield	6100^{+1600}_{-1500}	8580 ± 600

the results. Finally, since we have already corrected for efficiencies, the ratio of branching fractions is

$$R_{\eta'} = \frac{\mathcal{B}(D_s^+ \to \eta' e^+\nu)}{\mathcal{B}(D_s^+ \to \phi e^+\nu)} = \frac{6100^{+1600}_{-1500}}{8580 \pm 600} = 0.71^{+0.19+0.08}_{-0.18-0.10}, \quad (2)$$

where the first error is statistical, and the second is systematic. This systematic error includes: the uncertainty in the level of continuum charm background (10%), the uncertainty in the level of $B\bar{B}$ background (2.3%), the uncertainty in the ϕ and η' reconstruction efficiency (6.2%), the uncertainty in the level of feed down from D^+ decay (4.3%) and that due to the limited number of Monte Carlo events which were used for the efficiency estimates (6.0%). The systematic errors due to the uncertainty in the lepton identification efficiency and the uncertainty in the number of fake leptons mostly cancel (2.2%) since they are correlated in both analyses. Various background shapes have also been used to extract the number of η' and ϕ mesons. In all cases $R_{\eta'}$ changes by less than 4.2%, which is taken to be the systematic error. After combining these contributions in quadrature, the total systematic error is 15%.

Model predictions and measurements are listed in Table III including our new measurements. Our measurements of R_η and $R_{\eta'}$ are considerably higher than Scora's predictions with the modified ISGW model [21]. The prediction of Kamal *et al.* for R_η agrees well with our measurement whereas their prediction for $R_{\eta'}$ is somewhat higher than our measurement [25,26]. E653 reported an upper limit of $R_{\eta'}$ and a measurement of $R_\eta + R_{\eta'} = 3.9 \pm 1.6$ with the muon channels [9]. Our measurement of the ratio of pseudoscalar to vector rates for the D_s^+ semileptonic decay, *i.e.* $R_\eta + R_{\eta'} = 2.46 \pm 0.39 \pm 0.26$, is higher than the ratio found for the D^+ and D^0 semileptonic decay.

Having measured R_η and $R_{\eta'}$, we can extract the absolute branching fraction for $D_s^+ \to \phi e^+\nu$ by assuming that $\Gamma(D_s^+ \to Xe^+\nu) = \Gamma(D \to Xe^+\nu)$ and three decay modes $D_s^+ \to \phi e^+\nu$, $D_s^+ \to \eta e^+\nu$ and $D_s^+ \to \eta' e^+\nu$ almost saturate the D_s^+ semileptonic decay. This is

TABLE III. Summary of predictions and measurements.

Predictions and Measurements	R_η	$R_{\eta'}$	$R_\eta + R_{\eta'}$
Scora [21]	0.39	0.34	0.73
Kamal *et al.* [25,26]	$1.85 \pm 0.41 \pm 0.37$	$2.22 \pm 0.57 \pm 0.44$	$4.07 \pm 0.70 \pm 0.57$
E653 [9]		< 1.6 @90%C.L.	3.9 ± 1.6
This result	$1.74 \pm 0.34 \pm 0.24$	$0.71^{+0.19+0.08}_{-0.18-0.10}$	$2.46 \pm 0.39 \pm 0.26$

supported by the fact that $D \to Ke^+\nu$ and $D \to K^*e^+\nu$ almost saturate D semileptonic decay [11,27]. With these assumptions, we can write

$$\mathcal{B}(D_s^+ \to \phi e^+\nu) = \frac{1}{1 + R_\eta + R_{\eta'}} \times (1 - f_{cs} - f_{misc}) \times \mathcal{B}(D^0 \to Xe^+\nu) \times \frac{\tau_{D_s^+}}{\tau_{D^0}}. \quad (3)$$

where $\tau_{D_s^+}$ and τ_{D^0} are the D_s^+ and D^0 lifetimes, respectively. The factor f_{cs} includes all Cabibbo suppressed decay modes and f_{misc} includes $D_s^+ \to f_0(975)e^+\nu$ and other Cabibbo favored decays modes, which are estimated to be 0.05 ± 0.01 and 0.06 ± 0.04, respectively. We use CLEO II measurements for all quantities except the D_s^+ and D^0 lifetimes. In this way some of the systematic errors cancel and the problems associated with averaging the results from many different experiments are avoided. We find $1/(1 + R_\eta + R_{\eta'}) = 0.289 \pm 0.039$, and when this is combined with our measurement of $\mathcal{B}(D^0 \to Xe^+\nu) = (6.97 \pm 0.35)\%$ [27] and the E687 measurements, $\tau_{D^0} = (4.13 \pm 0.05) \times 10^{-13}$ s [23] and $\tau_{D_s^+} = (4.75 \pm 0.21) \times 10^{-13}$ s [24], we obtain $\Gamma(D_s^+ \to \phi e^+\nu) = (4.35 \pm 0.66) \times 10^{10}\ s^{-1}$ and $\mathcal{B}(D_s^+ \to \phi e^+\nu) = (2.06 \pm 0.33)\%$.

Combining our result for $\Gamma(D_s^+ \to \phi e^+\nu)$ with $\Gamma(D \to K^*e^+\nu) = (5.7 \pm 0.7) \times 10^{10}\ s^{-1}$ [11], we find $\Gamma(D_s^+ \to \phi e^+\nu)/\Gamma(D \to K^*e^+\nu) = 0.76 \pm 0.15$. The modified ISGW model [21], which is the only model up to date which predicts the measured value of $\mathcal{B}(D \to K^*e^+\nu)/\mathcal{B}(D \to Ke^+\nu)$ [3], predicts 1.00 for this ratio. Combining $\mathcal{B}(D_s^+ \to \phi e^+\nu)$ with our measurement of $\mathcal{B}(D_s^+ \to \phi e^+\nu)/\mathcal{B}(D_s^+ \to \phi\pi^+) = 0.54 \pm 0.06$ [26], we obtain $\mathcal{B}(D_s^+ \to \phi\pi^+) = (3.82 \pm 0.74)\%$. The branching fraction for $D_s^+ \to \phi\pi^+$ sets the scale for all D_s^+ hadronic branching fractions.

In conclusion, we have measured $\mathcal{B}(D_s^+ \to \eta e^+\nu)/\mathcal{B}(D_s^+ \to \phi e^+\nu) = 1.74 \pm 0.34 \pm 0.24$ and $\mathcal{B}(D_s^+ \to \eta' e^+\nu)/\mathcal{B}(D_s^+ \to \phi e^+\nu) = 0.71^{+0.19+0.08}_{-0.18-0.10}$. This is the first measurement of these quantities. Our measurement of the ratio of pseudoscalar to vector rates for the D_s^+ semileptonic decay disagrees with the modified ISGW model prediction. Our measurement of the ratio $\mathcal{B}(D_s^+ \to \eta' e^+\nu)/\mathcal{B}(D_s^+ \to \eta e^+\nu) = 0.41 \pm 0.13 \pm 0.05$ also disagrees with the prediction by the factorization model where we expect $\mathcal{B}(D_s^+ \to \eta' e^+\nu)/\mathcal{B}(D_s^+ \to \eta e^+\nu) = \mathcal{B}(D_s^+ \to \eta'\rho^+)/\mathcal{B}(D_s^+ \to \eta\rho^+) = 1.20 \pm 0.33$. We have made a relatively model independent estimate of $\mathcal{B}(D_s^+ \to \phi e^+\nu) = 2.06 \pm 0.33\%$. We have also estimated $\mathcal{B}(D_s^+ \to \phi\pi^+) = (3.82 \pm 0.74)\%$ by combining $\mathcal{B}(D_s^+ \to \phi e^+\nu)$ with our measurement of $\mathcal{B}(D_s^+ \to \phi e^+\nu)/\mathcal{B}(D_s^+ \to \phi\pi^+)$.

We gratefully acknowledge the effort of the CESR staff in providing us with excellent luminosity and running conditions. This work was supported by the National Science Foundation, the U.S. Dept. of Energy, the Heisenberg Foundation, the SSC Fellowship program of TNRLC, Natural Sciences and Engineering Research Council of Canada, and the A.P. Sloan Foundation.

REFERENCES

[1] Note that this is reverse of $\mathcal{B}(D \to \overline{K^*}\ell^+\nu)/\mathcal{B}(D \to K\ell^+\nu)$ which is usually quoted. We use this convention to be consistent with the ratios quoted in the text.

[2] For all states described, the charge conjugate state is also implied.

[3] Particle Data Group, K. Hikasa *et al.*, Review of Particle Properties, Phys. Rev. D **45** (1992) 1.

[4] N. Isgur *et al.*, Phys. Rev. D **39** (1989) 799.

[5] M. Wirbel *et al.*, Z. Phys. C **39** (1985) 627; and J.G. Körner and G.A. Schuler, Z. Phys. C **38** (1988) 511.

[6] T. Altomari and L. Wolfenstein, Phys. Rev. D **37** (1988) 681; and F.J. Gilman and R.L. Singleton, Phys. Rev. D **41** (1990) 142.

[7] V. Lubicz *et al.*, Phys. Lett. B **274** (1992) 415.

[8] C. Bernard *et al.*, Phys. Rev. D **43** (1991) 2140 and Phys. Rev. D **47** (1993) 998.

[9] E653 Collaboration, K. Kodama *et al.*, Phys. Lett. B **309** (1993) 483.

[10] CLEO Collaboration, Y. Kubota *et al.*, Nucl. Inst. and Meth. **A320** (1992) 66.

[11] CLEO Collaboration, J. Alexander *et al.*, Phys. Lett. B **317** (1993) 647.

[12] G.C. Fox and S. Wolfram, Phys. Rev. Lett. **41** (1978) 1581.

[13] D. Atwood and W.J. Marciano, Phys. Rev. D **41** (1990) 1736. Final-state radiation reduces the $D_s^+ \to \eta e^+\nu$ and $D_s^+ \to \phi e^+\nu$ acceptance by 2.5% and 1.1% respectively, and has a negligible effect in the muon channels.

[14] Fake leptons are either misidentified hadrons or muons from π^+ and K^+ decays in flight.

[15] J.G. Körner and G.A. Schuler, Z. Phys. C **46** (1990) 93. According to their calaculation, we estimate that the muon rates for $D_s^+ \to \eta\ell^+\nu$ and $D_s^+ \to \phi\ell^+\nu$ are 3% and 5%, respectively, lower than that for electrons.

[16] The phase-space background function has the form: $a \cdot (m - m_0)^\alpha \cdot e^{-\beta(m-m_0)}$, where m is the invariant mass of the K^+K^- pair. The parameter m_0 is obtained from a fit to the inclusive K^+K^- invariant mass distribution and fixed in fitting $D_s^+ \to \phi\ell^+\nu$ signal; α and β are free parameters.

[17] The ratio of the number of $D^+ \to \eta'\ell^+\nu$ events to the number of $D_s^+ \to \eta'\ell^+\nu$ events can be estimated as;

$$\frac{N(D^+ \to \eta'\ell^+\nu)}{N(D_s^+ \to \eta'\ell^+\nu)} = \frac{\sigma(D^+)}{\sigma(D_s^+)} \times \frac{\mathcal{B}(D^+ \to \eta'\ell^+\nu)}{\mathcal{B}(D_s^+ \to \eta'\ell^+\nu)} = \frac{\sigma(D^+)}{\sigma(D_s^+)} \times \frac{\Gamma(D^+ \to \eta'\ell^+\nu)}{\Gamma(D_s^+ \to \eta'\ell^+\nu)} \times \frac{\tau_{D^+}}{\tau_{D_s^+}}.$$

CLEO 1.5 measured $\sigma(D^+) \cdot \mathcal{B}(D^+ \to K^-\pi^+\pi^+)/\sigma(D_s^+) \cdot \mathcal{B}(D_s^+ \to \phi\pi^+) = (48.8 \pm 4.8)/(7.4 \pm 1.2) = 6.6 \pm 1.3$ [18]. Using our measurement of $\mathcal{B}(D^+ \to K^-\pi^+\pi^+) = (9.3 \pm 1.0)\%$ [19] and world average for $\mathcal{B}(D_s^+ \to \phi\pi^+)$ [20], we obtain $\sigma(D^+)/\sigma(D_s^+) = 2.5 \pm 0.8$. For $\Gamma(D^+ \to \eta'\ell^+\nu)/\Gamma(D_s^+ \to \eta'\ell^+\nu)$, Scora predicts $0.21 \cdot |V_{cd}/V_{cs}|^2$ for $\theta_P = -20°$ (θ_P is η-η' mixing angle) [21]. This corresponds to the form factor and phase space factor ratio of 0.93. Kamal *et al.* also predicts the ratio 0.93 [22]. Here, we assume $\Gamma(D^+ \to \eta'\ell^+\nu)/\Gamma(D_s^+ \to \eta'\ell^+\nu) = (0.2 \pm 0.1) \cdot |V_{cd}/V_{cs}|^2$ for our estimation. Using E687 measurements, $\tau_{D^+} = (10.48 \pm 0.19) \times 10^{-13}$ s [23] and $\tau_{D_s^+} = (4.75 \pm 0.21) \times 10^{-13}$ s [24], we obtain;

$$f_{FD} \equiv \frac{N(D^+ \to \eta'\ell^+\nu)}{N(D_s^+ \to \eta'\ell^+\nu)} = (2.5 \pm 0.8) \times (0.2 \pm 0.1) \times 0.051 \times (2.2 \pm 0.1) = 0.06 \pm 0.04.$$

[18] CLEO Collaboration, R. Armer *et al.*, Phys. Rev. D **44** (1991) 3583.

[19] CLEO Collaboration, R. Balest *et al.*, Phys. Rev. Lett. **72** (1993) 2328.

[20] F. Muheim and S. Stone, preprint HEPSY 93-3, to appear in Phys. Rev. D. Using three different model dependent methods, they estimate $\mathcal{B}(D_s^+ \to \phi\pi^+) = (3.5 \pm 0.6)\%$.

[21] D. Scora, Ph.D. thesis, University of Toronto, 1993. We take the predictions for $\theta_P = -20°$.

[22] A.N. Kamal *et al.*, submitted to Physical Review.

[23] E687 Collaboration, P.L. Frabetti *et al.*, Phys. Lett. B **323** (1994) 459.

[24] E687 Collaboration, P.L. Frabetti *et al.*, Phys. Rev. Lett. **71** (1993) 827.

[25] A.N. Kamal *et al.*, Phys. Rev. D **49** (1994) 1330. Combining the factorization hypothesis with the measurements of $\mathcal{B}(D_s^+ \to \eta\rho^+)/\mathcal{B}(D_s^+ \to \phi\pi^+)$ and $\mathcal{B}(D_s^+ \to \eta'\rho^+)/\mathcal{B}(D_s^+ \to \phi\pi^+)$, Kamal *et al.* predict $\mathcal{B}(D_s^+ \to \eta e^+\nu)/\mathcal{B}(D_s^+ \to \phi\pi^+) = 1.00 \pm 0.19 \pm 0.20$ and $\mathcal{B}(D_s^+ \to \eta' e^+\nu)/\mathcal{B}(D_s^+ \to \phi\pi^+) = 1.20 \pm 0.27 \pm 0.24$. We combine the predictions of Kamal *et al.* and the recent CLEO measurement for $\mathcal{B}(D_s^+ \to \phi e^+\nu)/\mathcal{B}(D_s^+ \to \phi\pi^+)$ [26] to reach the predictions for R_η and R'_η quoted in the text.

[26] CLEO Collaboration, F. Butler *et al.*, Phys. Lett. B **324** (1994) 255.

[27] CLEO result presented at the APS meeting in April, 1994.

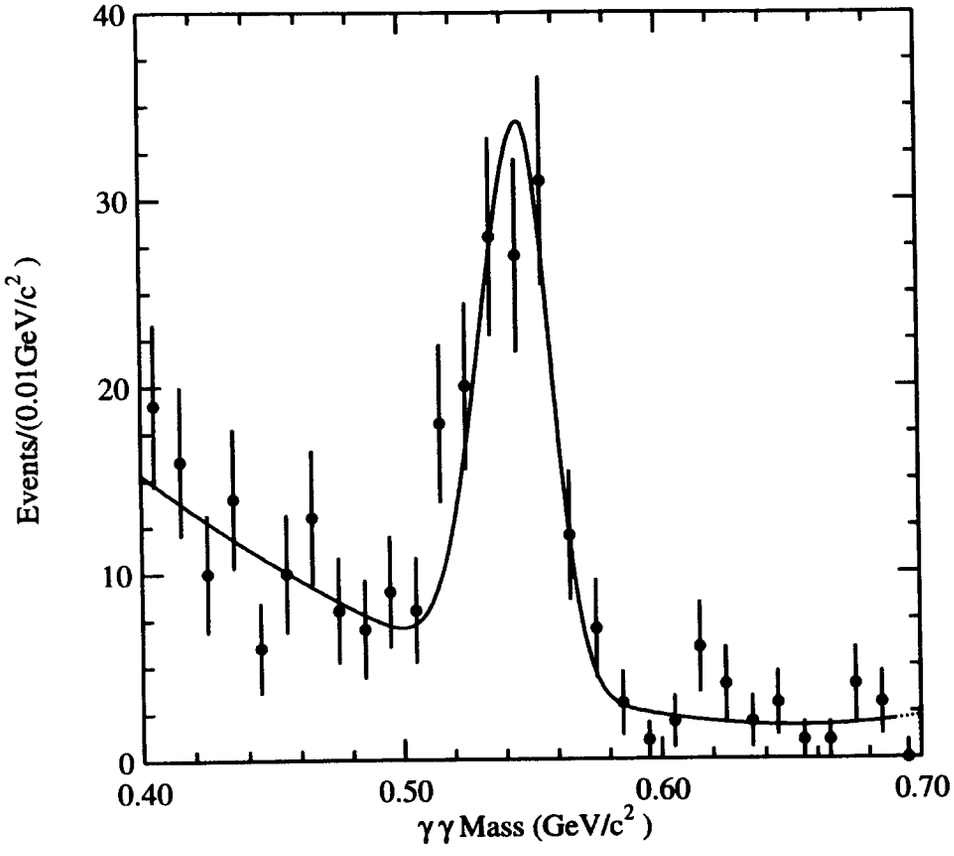

FIG. 1. The $\gamma\gamma$ invariant mass distribution for $D_s^+ \to \eta\ell^+\nu$ candidates. The curve is the fit to the invariant mass distribution.

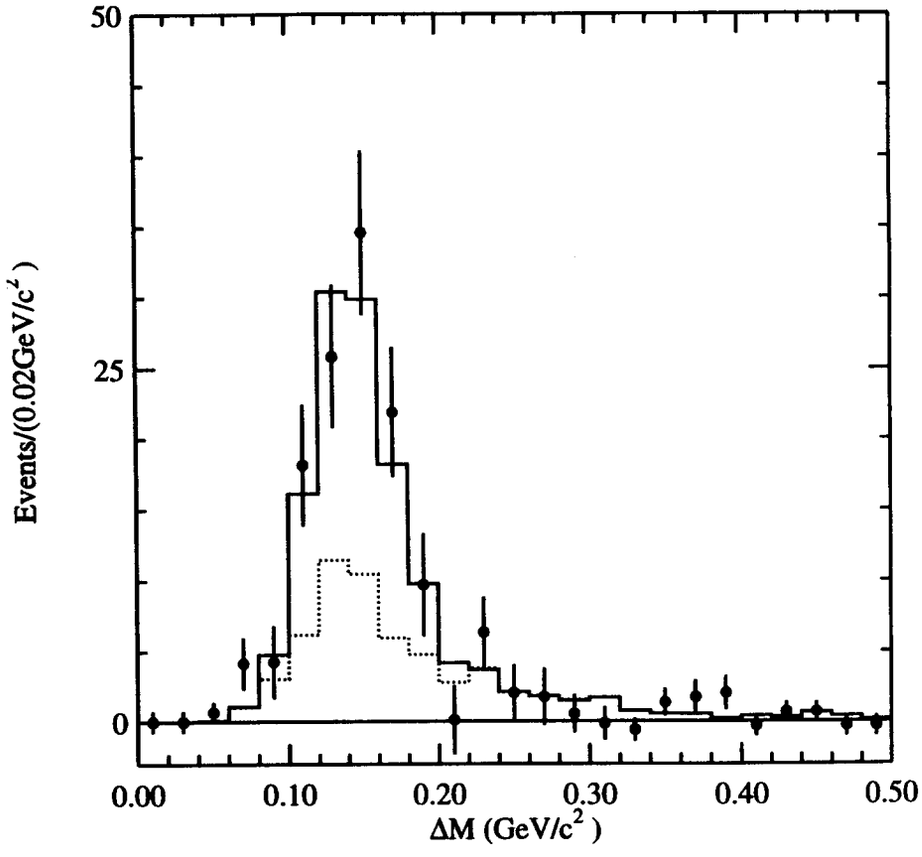

FIG. 2. Pseudo mass difference between D_s^{*+} and D_s^+ for $D_s^+ \to \eta\ell^+\nu$ candidates. The solid circles represent the candidates in each ΔM bin. The solid histogram shows the sum of the simulated signal shape and the predicted background. The dashed histgram shows the predicted background.

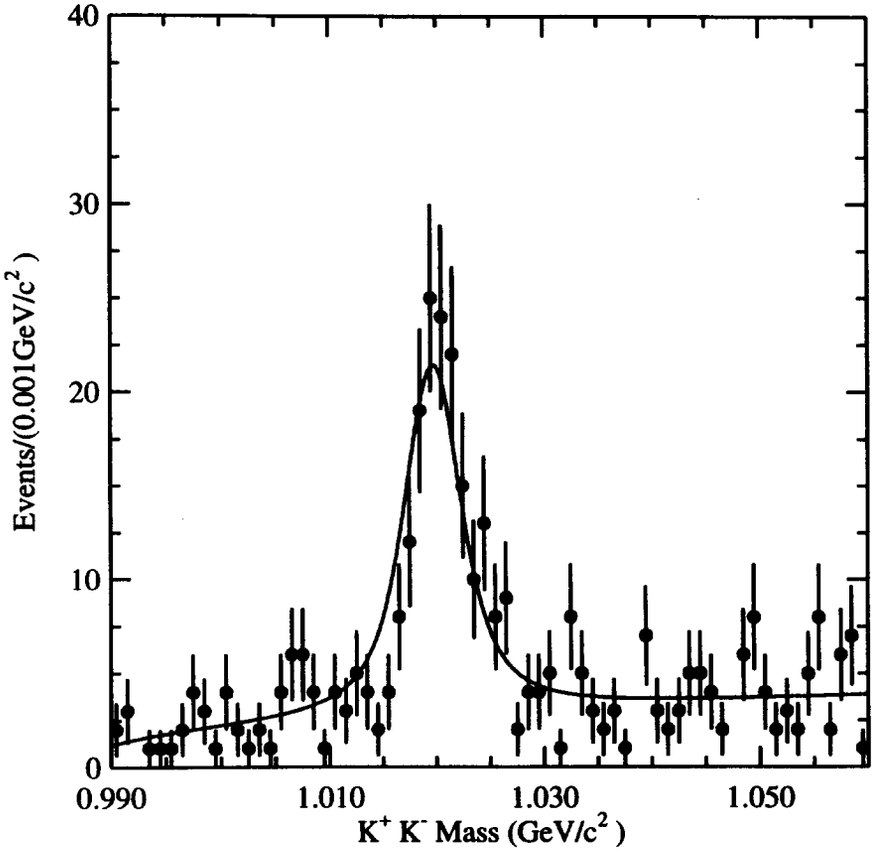

FIG. 3. The K^+K^- invariant mass distribution for $D_s^+ \to \phi\ell^+\nu$ candidates. The curve is the fit to the invariant mass distribution.

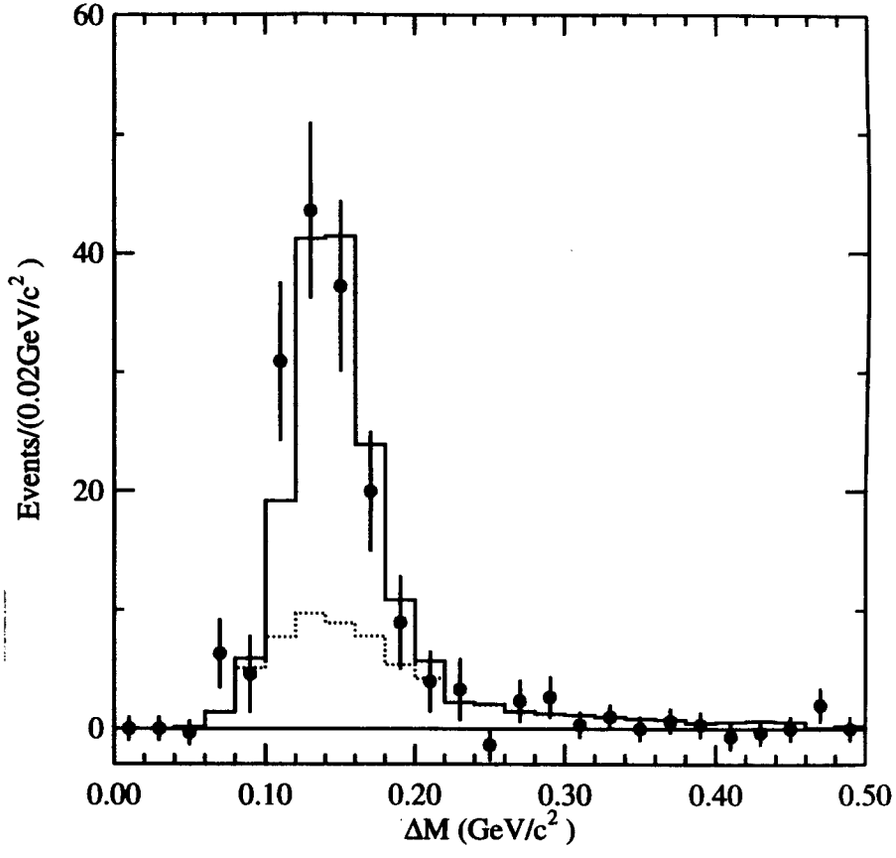

FIG. 4. Pseudo mass difference between D_s^{*+} and D_s^+ for $D_s^+ \to \phi\ell^+\nu$ candidates. The solid circles represent the candidates in each ΔM bin. The solid histogram shows the sum of the simulated signal shape and the predicted background. The dashed histgram shows the predicted background.

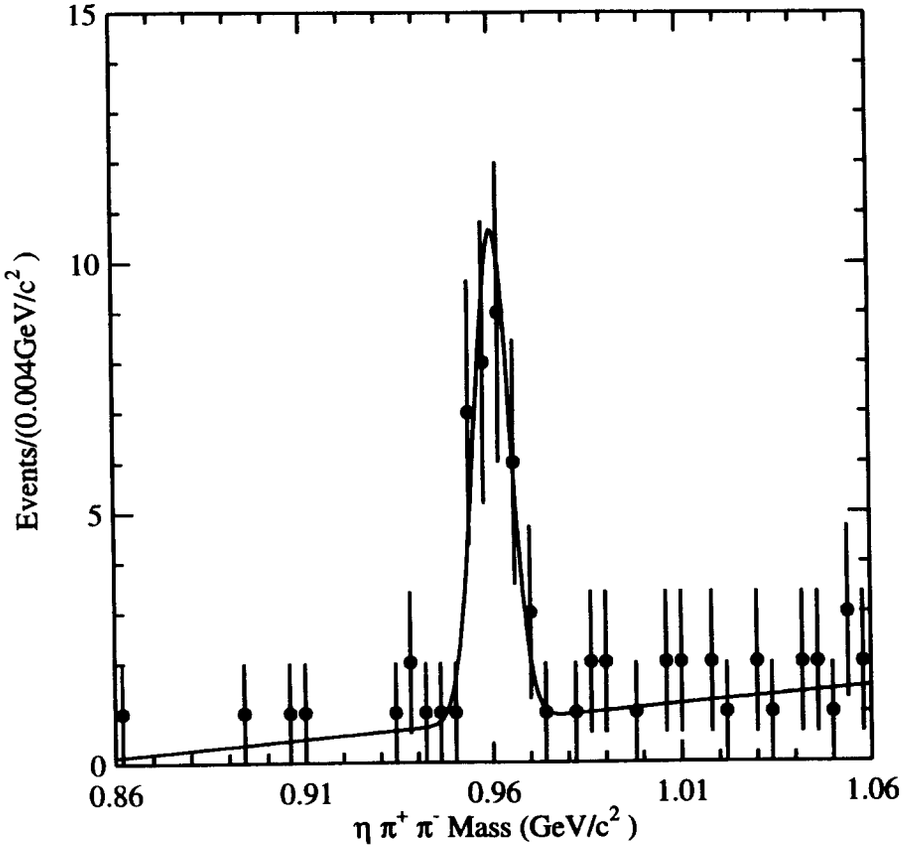

FIG. 5. The $\eta\pi^+\pi^-$ invariant mass distribution for $D_s^+ \to \eta'\ell^+\nu$ candidates. The curve is the fit to the invariant mass distribution.

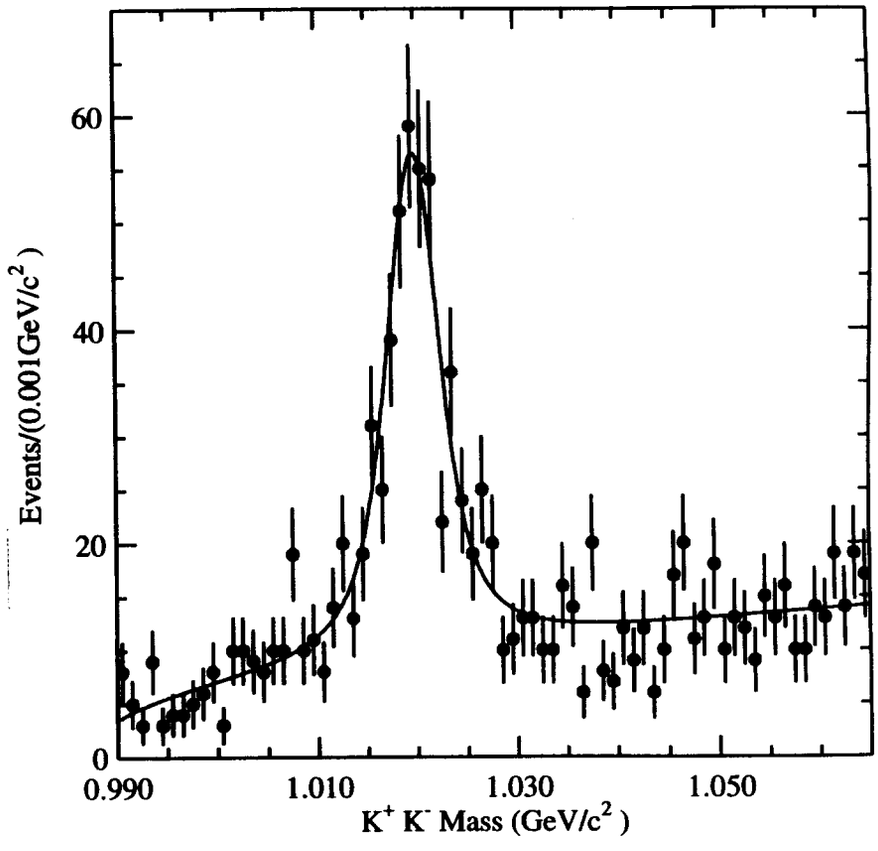

FIG. 6. The K^+K^- invariant mass distribution for $D_s^+ \to \phi\ell^+\nu$ candidates. The curve is the fit to the invariant mass distribution.